Journal of Oral Science, Vol. 62, No. 3, 259-264, 2020

Original article

Wettability and pre-osteoblastic behavior evaluations of a dense bovine hydroxyapatite ceramics

Luara A. Pires[1)], Camila R. de Meira[2)], Cintia K. Tokuhara[3)], Flávia A. de Oliveira[3)], Vanessa B. Dainezi[4)], Marcia S. Zardin Graeff[3)], Carlos A. Fortulan[2)], Rodrigo C. de Oliveira[3)], Regina M. Puppin-Rontani[4)], and Ana Flávia S. Borges[1)]

[1)] Department of Operative Dentistry, Endodontics and Dental Materials, Bauru School of Dentistry, University of São Paulo, Bauru, SP, Brazil
[2)] Department of Mechanical Engineering, São Carlos School of Engineering, University of São Paulo, São Carlos, SP, Brazil
[3)] Department of Biological Sciences, Bauru School of Dentistry, University of São Paulo, Bauru, SP, Brazil
[4)] Department of Pediatric Dentistry, Faculty of Dentistry of Piracicaba, State University of Campinas, Piracicaba, SP, Brazil

(Received January 8, 2019; Accepted July 4, 2019)

Abstract: In this study, the wettability, cell viability, and roughness of an experimental dense bovine hydroxyapatite [$Ca_{10}(PO_4)_6(OH)_2$] ceramic block were evaluated so that, in the future, it could be used as a base material for dental implants. The results to commercial zirconia and a commercially pure titanium (Ti) alloy were compared. The surface roughness and contact angles were measured. An *in vitro* evaluation was conducted by means of tests in which pre-osteoblastic MC3T3-E1 cells were placed in indirect and direct contact with these materials. For cell viability, a 3-(4,5-dimethylthiazol-2-yl)-2,5-diphenyl tetrazolium bromide (MTT) assay and crystal violet test were conducted. A qualitative analysis was conducted using variable pressure scanning electron microscopy (SEM). No statistically significant differences were observed in wettability and roughness tests among the groups. In both the MTT assay and crystal violet test, all groups demonstrated satisfactory results without cytotoxicity. SEM showed cell adhesion and cell proliferation results on the material surfaces after 24 h and 48 h. In conclusion, this dense $Ca_{10}(PO_4)_6(OH)_2$ ceramic can be considered as a potential biocompatible material.

Keywords; biocompatible materials, cell adhesion, cell survival, hydroxyapatite, wettability

Introduction

Cattle industry activity has great socio-economic importance in Brazil, but there is environmental concern about the impact caused by the generation of solid waste and liquids (e.g., bones, fat, offal, manure, and blood) that pollute the environment after the animal is slaughtered, defiling river water, soil, and air, thus causing damage to health [1]. The recovery of these by-products, such as bovine bone, can contribute significantly to reductions of the negative impacts on the environment [2].

Because of the great quantity and low cost of bovine bone, and considering the environmental concerns, many companies have been producing biomaterials using this material. These bones are the source of hydroxyapatite [$Ca_{10}(PO_4)_6(OH)_2$], which has a mineral composition and structure similar to natural bone and is a major constituent of the mineral aspect of human bones and teeth. Therefore, $Ca_{10}(PO_4)_6(OH)_2$ has features such as biocompatibility, osteoconductivity, and bioactivity [3], and it is known to unite chemically and directly to the bone when implanted [4].

With the advancement and improvement of ceramic material properties, they have become of great interest in the medical and dental fields. Bioceramics are classified as biomaterials and are used especially in the repair, reconstruction, and replacement of bone portions affected by pathology or trauma. A bioceramic with potential for dental implants is $Ca_{10}(PO_4)_6(OH)_2$ ceramic (HC), which is a type of calcium phosphate bioceramic. Different forms of HC have applicability in the biomedical field for the repair or replacement of bone tissues. Dense $Ca_{10}(PO_4)_6(OH)_2$-based materials with adequate mechanical properties are often used in tooth formations to minimize alveolar resorption, and they are used in particulate formations as individual implants. These materials are also used as fillers for bony defects and as fillers in association with the placement of metal implants. When considering a biomaterial to be used in implants or bone grafts, factors such as biocompatibility, osteogenic properties, bioactivity, and its mechanical properties, including its functionalities, need to be studied [5,6]. The brittle nature, low-fracture toughness, and hardness of sintered HAP-based bioceramics often limit the use of these materials in some load-bearing clinical applications [7]. However, improvements in the mechanical properties of HAP-based bioceramic materials were achieved by controlling the grain size, shape, and pore size [8-11].

In studies of biomaterials, *in vitro* tests characterize the cellular responses to the studied substrate. An *in vitro* study is also able to produce a fast response and allows evaluation of factors such as cytotoxicity, biocompatibility, proliferation, and cell viability. Its advantages, compared with *in vivo* studies, include the speed of results, reproducibility, high sensitivity, low cost, and good control of variables [12].

Implant surface quality is a major factor in biocompatibility. When the surface of the implanted biomaterial is exposed to tissue fluids, an initial interaction occurs between the living bone and tissue and the implant surface [13,14]. Material surface properties are, therefore, important factors in the interfacial phenomena such as protein adsorption and the cellular behavior of biomaterials [15-18]. The wettability of the surfaces can be quantified by the contact angle of a liquid on a solid substrate. The contact angle is the angle of intersection of a line tangent to the liquid and the surface of the solid that it contacts. This angle is characteristic of the substances in the system because of the surface tension of the liquid and the surface energy of the solid, which is modified by certain properties, such as roughness. Studies have shown that hydrophilic surfaces tend to increase the initial phases of cell adhesion, differentiation, proliferation, and mineralization of bone compared with hydrophobic surfaces [19-23].

In this study, wettability and roughness were measured, and biological behaviors were evaluated by means of *in vitro* pre-osteoblastic cell viability. They were measured qualitatively on dense HC material and were then compared with one kind of zirconia stabilized by yttria and a commercially pure Ti alloy, which are materials that are currently used in the manufacture of dental implants.

Materials and Methods

Manufacturing and preparation of specimens

Obtaining $Ca_{10}(PO_4)_6(OH)_2$ powder

$Ca_{10}(PO_4)_6(OH)_2$ was obtained from bovine femurs from animals that were screened by the Brazilian System of Identification and Certification of Bovine and Bubaline (Sisbov).

The processing of bone tissue to obtain $Ca_{10}(PO_4)_6(OH)_2$ followed standard operating procedures of the company Criteria Industry and Trade of Medicinal Products and Dental Ltda. (São Carlos, SP, Brazil) and was

Correspondence to Dr. Ana Flávia S. Borges, Department of Operative Dentistry, Endodontics and Dental Materials, Bauru School of Dentistry, University of São Paulo, Avenue Doctor Otávio Pinheiro Brisola 9-75, Bauru, São Paulo 17.012-901, Brazil
Fax: +55-14-981049985 E-mail: afborges@fob.usp.br

Color figures can be viewed in the online issue at J-STAGE.
doi.org/10.2334/josnusd.19-0007
DN/JST.JSTAGE/josnusd/19-0007

Table 1 Components, proportions, and functions of dense bovine hydroxyapatite ceramic

Component	Proportion (%)	Function
HA (hydroxyapatite)	30% (total volume)	Powder
PVB (polyvinyl butyral)	0.05% (HA weight)	Binder
PABA (para-aminobenzoic acid)	2% (HA weight)	Dispersant
Isopropyl alcohol	70% (total volume)	Solvent

carried out at the premises to avoid contamination and ensure the quality of the material. The samples were treated with thermochemical processes to remove organic matter. Samples of the extracted material were sent to a laboratory accredited by the Ministry of Health for analysis to demonstrate the absence of heavy metals in the composition of the bone and verify the absence of biological contamination. Once the results of the analysis showed no heavy metals in the composition of the bone tissue and the absence of cytotoxicity, the samples were released to be used in the production of $Ca_{10}(PO_4)_6(OH)_2$ granules.

For the characterization of bovine $Ca_{10}(PO_4)_6(OH)_2$, X-ray diffraction (Multiflex, Rigaku, Tokyo, Japan) and Fourier Transform Infrared (IRAffinity 1, Shimadzu, Kyoto, Japan) spectroscopy were performed. The data were compared with standard values for $Ca_{10}(PO_4)_6(OH)_2$ powder (Sigma-Aldrich, St. Louis, MO, USA). Wavelength dispersion X-ray fluorescence (RIX3000, Rigaku) analysis was also performed to verify that the chemical composition was in accordance with ASTM F1185-03, which determined the maximum allowed concentrations of heavy metals to $Ca_{10}(PO_4)_6(OH)_2$ obtained from an animal origin. The best temperature calcination of bovine bone powders was 900°C.

Preparation of dense bovine HC

The components used in the manufacture of $Ca_{10}(PO_4)_6(OH)_2$ discs are listed in Table 1.

$Ca_{10}(PO_4)_6(OH)_2$ was ground to reduce the size of the particles and increase the reactivity between them, thereby reducing the temperature and time necessary for sintering the final porosity of the HC. Polyvinyl Butyral (PVB; Butvar B98, Solutia Inc., St. Louis, MO, USA) was added to provide plasticity and strength after the formation process. A polyethylene jar that was 85 mm in height, 300 cm^3 in volume, and loaded with 40 vol% (500 g) milling elements, was used for milling and obtaining the submicrometric powder, which was, in this case, 3Y zirconia spheres that were 10 mm in diameter. This resulted in a useful volume of 100 mL. The jar was charged with a barbotine at a concentration of 30 vol% solids and placed in a ball mill at a speed of 104 rad s^{-1} for 24 h, 48 h, 72 h, and 96 h, followed by vibratory milling for 24 h to 48 h.

The obtained specimens were placed in two types of mills in an alcoholic medium. In the first milling, the jar was charged with 30 vol% $Ca_{10}(PO_4)_6(OH)_2$, 70 vol% isopropyl alcohol, and 0.05 wt% para-aminobenzoic acid (PABA; Vetec Química Fina, Duque de Caxias, Brazil). It was then was placed for 96 h in a ball mill. After this time, 1.2 wt% of PVB was added based on the weight of the $Ca_{10}(PO_4)_6(OH)_2$, which was mixed and homogenized in a ball mill for 2 h. The jar was discharged, and the barbotine was dried with a hot air blower at about 80°C.

All the prepared powder was granulated and classified with stitches (sieves) stainless steel # 200 mesh ≤75 μm to obtain an average size of 0.35 μm. Cylindrical forms that were 15 mm in diameter and 4 mm thick were obtained from the powders with a uniaxial pressure of 100 MPa for 30 s. The surfaces of the discs were ground with silicon carbide abrasive papers with #240, #320, #400, #600, and #1,500 mesh, and the discs were then polished with 9 μm to 1 μm diamond pastes.

$Ca_{10}(PO_4)_6(OH)_2$ was sintered to consolidate the particles, promote densification (reduced porosity and increased bulk density), and increase the mechanical strength. This was performed in a Lindberg Blue/M furnace chamber at an ambient air temperature increased to 160°C at a heating rate of 2.7°C/min. The temperature was then changed to 600°C at 4°C/min, then up to 1,100°C at 5°C/min, and finally increased to the maximum temperature (1,300°C) at 6°C/min for 120 min followed by threshold furnace cooling to ambient temperature [24].

Commercially pure Ti

Ti was provided in cylindrical bars by Sandinox (Sorocaba, Brazil). The cylinders were 13 mm in diameter. A precision cutting machine (IsoMet 1000; Buehler, Lake Bluff, IL, USA) was used to cut cylinders to a thickness of 4.5 mm.

For finishing and polishing, the surface discs were fixed with impression composite on a glass slide in pairs to perform the polishing step with granulations of 800, 1,000, and 1,200 using a precision microgrinding system (Exakt 400 CS; Exakt, Norderstedt, Hamburg, Germany).

Zirconia stabilized by yttria ZirCAD (Z-CAD)

Pre-sintered zirconia blocks stabilized by yttrium oxide IPS e.max Z-CAD (IvoclarVivadent, Liechtenstein) for a CAD/CAM system were cut into cylindrical forms of 13 mm in diameter. The cylinders were cut on the cutting machine to a thickness of 5.7 mm.

The finishing was performed with sandpaper of 1,000 and 1,200 granulations using an Exakt CS 400 machine. The polishing was done with granulated felt discs with average, fine and extra-fine diamond paste and by means of a semi-automatic polishing Ecomet 4 (Buehler).

Thereafter, the disks were washed with distilled water in a computerized ultrasonic vat (USC 700, Unique, São Paulo, Brazil) and sintered at 1,500°C for about 8 h.

Previous tests with bovine dense HC

Meira et al. observed that the maximum density at 1,300°C was obtained for powder milled in an alcoholic medium in a ball mill with a smaller particle diameter (0.35 μm) in a vibratory mill. Under these conditions, for a three-point flexural strength test, they obtained values close to 100 MPa, which were above the values reported in the literature. The increase in Vickers hardness and a lower standard deviation (483 ± 25) confirmed the idealization of grinding in an alcoholic medium. The combination of the results of high densification, small grain size, chemical stability of the $Ca_{10}(PO_4)_6(OH)_2$ phase, and high hardness was decisive for the sintering decision at a temperature of 1,300°C.

Surface roughness

Six discs of each material were prepared. Their surface roughness was measured using a profilometer (Surfcorder SE1700, Kosaka Corp, Tokyo, Japan). Three measurements were made on the surfaces of each disc at different points, and an average and standard deviation were calculated.

Contact angle

In this test, six discs of each material were also prepared. Distilled water was dropped onto each of the discs (Fig. 1), and the contact angles were measured using an automated contact-angle-measuring goniometer (Ramé-Hart 500, Ramé-hart Instrument Co., Succasunna, NJ, USA), which included a video camera. Each value was obtained from measurements of the left and right angles of each droplet deposited on the surfaces of the materials to provide an average and standard deviation.

Cell culture

In this study, two discs were used for viability testing by indirect contact, and 6 discs were used for scanning electron microscopy (SEM) analysis of each material.

Pre-osteoblastic MC3T3-E1 cells of murine lineage originating from the American Type Culture Collection (Manassas, VA, USA) were grown in alpha Minimum Essential Medium (α-MEM; Nutricell, Campinas, Brazil) containing the nucleosides cytidine, adenosine, deoxycytidine, deoxyguanosine, deoxyadenosine, thymidine, guanosine, and uridine (Sigma-Aldrich) and 10% fetal bovine serum (FBS; Sigma-Aldrich). Cells of the 14th passage were used in the experiments [25].

Cell viability

The *in vitro* tests for cytotoxicity analysis using methods of 3-(4,5-dimethylthiazol-2-yl)-2,5-diphenyl tetrazolium bromide (MTT; Sigma-Aldrich) reduction and incorporation by crystal violet were performed according to the ISO 10993-5 standard [26].

Before the discs were weighed to assess the amount to be included in each medium, they were washed in a computerized ultrasonic vat with 100% methanol and distilled water and then autoclaved.

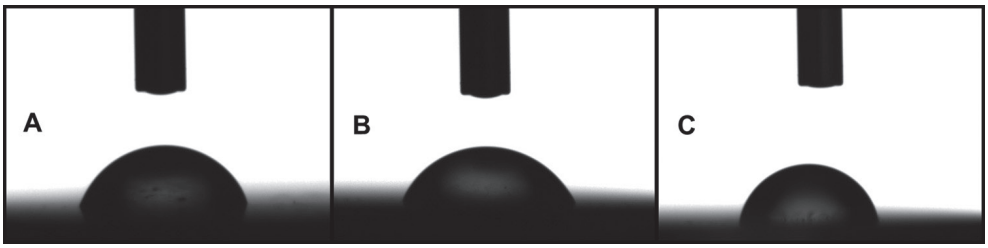

Fig. 1 Contact angle between the distilled water drop and the substratum: (A) hydroxyapatite ceramic; (B) zirconia ZirCAD; and (C) commercially pure titanium

Table 2 Values of surface roughness (μm)

Groups	Mean ± standard deviation
Hydroxyapatite ceramic	1.68 ± 0.58 a
Zirconia ZirCAD	1.42 ± 0.31 a
Commercially pure titanium	1.52 ± 0.40 a

Table 3 Values of contact angles (°)

Groups	Mean ± standard deviation
Hydroxyapatite ceramic	65.3 ± 8.3 a
Zirconia ZirCAD	66.5 ± 8 a
Commercially pure titanium	70.3 ± 8.2 a

For each 1 g of material, 10 mL of α-MEM medium was used to prepare the extract, and the solution was then incubated at 37°C for 48 h before being placed in culture plates to achieve the desired confluency. Two discs of each group were placed within the medium.

The cell plating was performed in 12 plates with 96 microwells per plate at a density of 2×10^3 cells/well in α-MEM with 10% FBS in contact with extracts of the material previously prepared. In each plate, eight wells of each group were filled with diluted extracts at 50%.

An MTT reduction test and crystal violet test were selected for the *in vitro* evaluation of cytotoxicity. Both tests were performed in duplicate at periods of 24 h, 48 h, and 72 h after plating. The wells that were used as a positive control (C 10%) were filled with α-MEM medium with 10% FBS, corresponding to 100% cell viability. In the wells for the negative control (C 1%), α-MEM medium and 1% phenol were added to produce toxicity.

The groups were named HC, HC 50% (HC diluted to 50%), Ti (commercially pure Ti), Ti 50% (commercially pure Ti diluted to 50%), Z-CAD (Z-CAD zirconia), and Z-CAD 50% (Z-CAD zirconia diluted to 50%).

MTT assay

Reduction of the colorimetric MTT assay was used to analyze the mitochondrial activity of the cells [27]. MTT, a yellowish salt that is soluble in water, was reduced by dehydrogenase activity in a compound called formazan, and this created an insoluble purple coloration. This reduction only occurs in living cells.

After removal of the medium and washing with phosphate-buffered saline (PBS), each microwell was filled with 110 μL solution containing 0.5 mg/mL of MTT, and the plates were incubated in 5% CO_2 for 4 h at 37ºC in the dark. After the supernatant was removed and the solution was discarded, 200 μL of dimethyl sulfoxide was added to each microwell. Cytotoxicity was assessed by spectrophotometrically measuring the absorbance using an ELISA reader (Fluostar Optima; BMG Labtech, Offenburg, Germany) at a wavelength of 570 nm.

Crystal violet colorimetric test

The crystal violet colorimetric test assessed the cell density by means of DNA staining with a crystal violet dye. It was performed at the same time as the MTT test.

The medium was removed from the microwells and were washed with PBS. Methanol 100% was added for 10 min. The methanol was then removed, and the cells were stained with 0.2% crystal violet diluted in 2% ethanol and then left for 3 min. The stain was removed, and the wells were washed again with PBS. Sodium citrate 0.05 mol/L in 50% ethanol was added and acted for 10 min. Finally, as in the MTT assay, reading of the optical densities was performed in the microwells with an ELISA reader at a wavelength of 570 nm.

Statistical analysis

The data obtained from the indirect viability experiments were expressed as percentages of the total number of viable cells in each microwell calculated in comparison to the positive control group (C 10%) to normalize the results.

The mean and standard deviation of the percentage values for each material and period were calculated and statistically analyzed with Kolmogorov-Smirnov and Shapiro-Wilk normality tests. The homogeneity of variance was analyzed with a Levene test. Subsequently, the data were analyzed with a one-way parametric ANOVA ($\alpha = 0.05$), followed by Tukey's test, using Graph Pad Prism version 4.00 for Windows (Graph Pad Software, San Diego, CA, USA). Statistical differences were considered significant when $P < 0.05$.

SEM

For this test, six discs of each group were washed in a computerized ultrasonic vat with 100% methanol and distilled water and were then autoclaved.

First, the cultured cells were evaluated using an optical microscope to verify confluence, and then they were added to the Neubauer chamber for cell counting with a microscope.

Two 24-well plates were used to accommodate three discs from each group for 24 h and three discs for 48 h. The pre-osteoblastic cells previously cultured in α-MEM were placed on the discs at a density of 2×10^4 cells/well. The wells were filled with α-MEM to cover the discs, and the plates were incubated for 24 h and 48 h in 5% CO_2 at 37°C. Later, the medium was delicately removed by suction and then washed with PBS to remove non-adherent cells.

For each period, adherent cells were fixated in osmium tetroxide vapor. In a gas exhaust hood, the discs on the glass slides were placed in petri dishes lined with watered filter paper (humid chambers). Then, 1 mL of osmium tetroxide 2% was collected and placed in a small plastic lid and inserted into the petri dishes together with the discs. Plates were sealed and maintained in the chapel for 48 h, which was the period necessary to volatilize the osmium tetroxide, promoting cell fixation on the discs.

After fixation for 48 h, the petri dishes containing discs were opened and placed in the desiccator for 3 h. Thereafter, the discs were fixed in stubs with nail polish. Next, they were metalized by depositing gold in the sputter device (Denton Vacuum Desk IV, CTC).

To evaluate the adhesion of cells, the images were generated using SEM with variable pressure (APEX Express, APEX Corporation, Delmont, PA, USA).

Results

Surface roughness

No statistically significant differences were observed among the groups regarding surface roughness (Table 2).

Contact angle

No statistically significant differences were observed among the groups regarding the contact angle (Table 3). All contact angles generated by the drop of distilled water on the surface of the materials were smaller than 90°, which characterized the materials as hydrophilic.

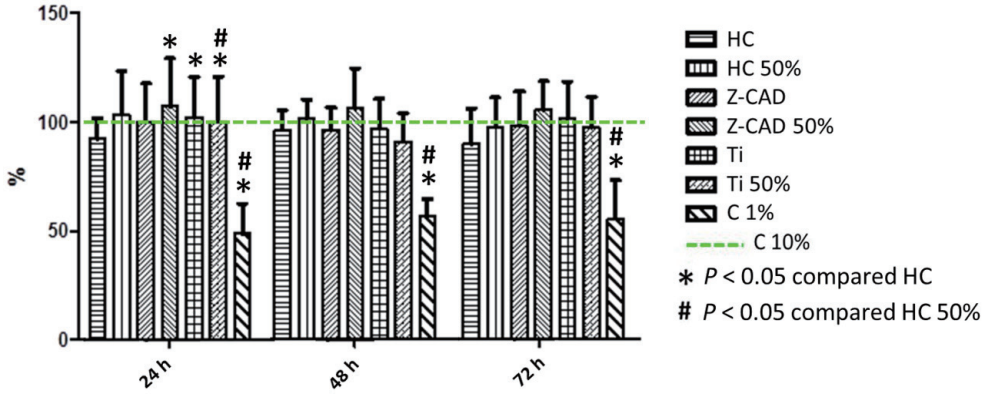

Fig. 2 Intergroup evaluation of cell viability using a MTT assay over 24 h, 48 h, and 72 h for groups HC, HC 50%, Z-CAD, Z-CAD 50%, Ti, Ti 50%, and C1%, normalized to the values of the positive control group (C 10%), considering 100%. Data are expressed as the mean and standard deviation.

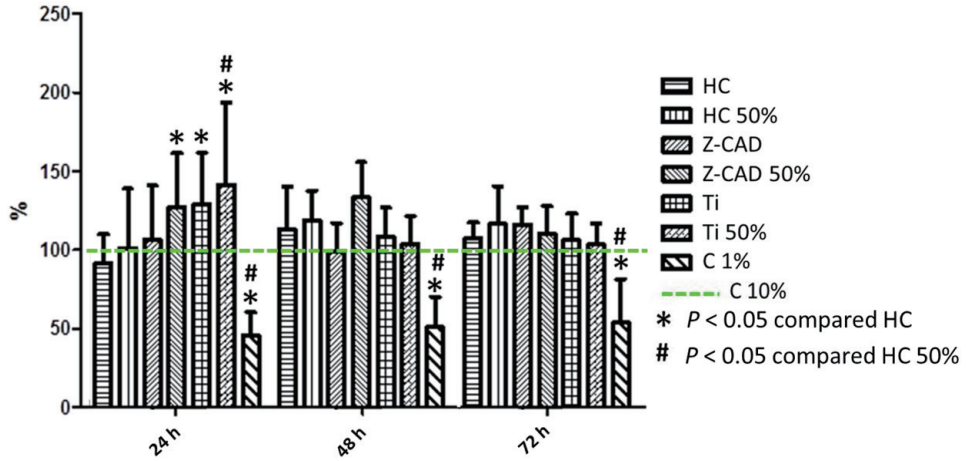

Fig. 3 Intergroup evaluation of cell viability using a crystal violet assay over 24 h, 48 h, and 72 h for groups HC, HC 50%, Z-CAD, Z-CAD 50%, Ti, Ti 50%, and C1%, normalized to the values of the positive control group (100%). Data are expressed as mean and standard deviation.

Cell viability

The optical density reading of the material held in the ELISA reader was compared with the mean cell positive control (α-MEM + 10% FBS), considering 100% cell viability.

Quantitative analysis was carried out so that the data were converted to a percentage relative to the positive control group, considering 100%. Thus, the absorbance percentages of the groups were compared with each other statistically within each period.

MTT

In a 24-h period, the viability values (%) of the evaluated groups were all close to the positive control group (100%), except for the negative control group (48.82% ± 13.59%), demonstrating biocompatibility of all samples studied. In 48 h, the viability profile continued to have values close to the controls (100%), and the negative group was similar to the previous period (56.34 ± 7.97%). The same was observed at 72 h, confirming the biocompatibility of the materials and the negative control as a cell growth inhibitor (55.12% ± 17.66%).

In 24 h, comparing the results with the HC (*), there was a higher significant difference ($P < 0.05$) for Z-CAD 50%, Ti and Ti 50% and a lower significant difference for the C 1% groups. Compared with HC 50% (#), the difference was greater for Ti 50% and lower for C 1%. At 48 h, both HC and HC 50% were only significantly higher than the negative group, C 1%. Within 72 h, as well as 48 h, there were minor differences in the control group statistics C 1% compared with HC and HC 50% (Fig. 2).

Crystal violet

It can be observed that all groups tested were well above the cell viability index of cytotoxicity, depicted by the negative controls (C 1%) at 24 h (45.51% ± 14.83%), 48 h (50.75% ± 19.35%), and at 72 h (53.64% ± 27.59%), indicating that these samples did not show any cytotoxic effects, which was similar to the test with MTT.

At 24 h, the groups with significant differences from HC (*) were Z-CAD 50%, Ti, and Ti 50%, with higher values, and C 1%, with a lower value. Compared with HC 50% (#), the Ti 50% group had greater significance, while the C 1% was lower. At 48 h, both HC and HC 50% were significantly higher than the negative group, C 1%. There were no differences in the other groups. At 72 h, there were lower statistical differences between the negative control group, C 1%, and the CH and CH 50% groups (Fig. 3).

SEM

The images were analyzed by SEM using variable pressure after 24 h and 48 h of plating.

In 24 h, it was verified that the cells were adhered to the surfaces of the materials. For HC (Fig. 4A), there seemed to be fewer cells than for the other materials. The cells had rounded features on the Ti surface (Fig. 4B), while in Z-CAD zirconia (Fig. 4C), the early formation of filopodial extensions (arrows) was observed.

In the analysis, we observed that, after 48 h, cells were more defined as to the morphological characteristics of HC (Fig. 5A). The nucleus and cytoplasm were more evident. These characteristics were similar to those found in cells that adhered on the Ti surface (Fig. 5B). In Z-CAD zirconia (Fig. 5C), the process of issuance of filopodial extensions in the cells became more evident.

Discussion

Hydrophilic surfaces tend to increase in the early stages of cell proliferation, cell adhesion, cell differentiation, and mineralization of bone compared with hydrophobic surfaces. The results of this study, in which contact angles of the materials were smaller than 90°, showed the bioc-

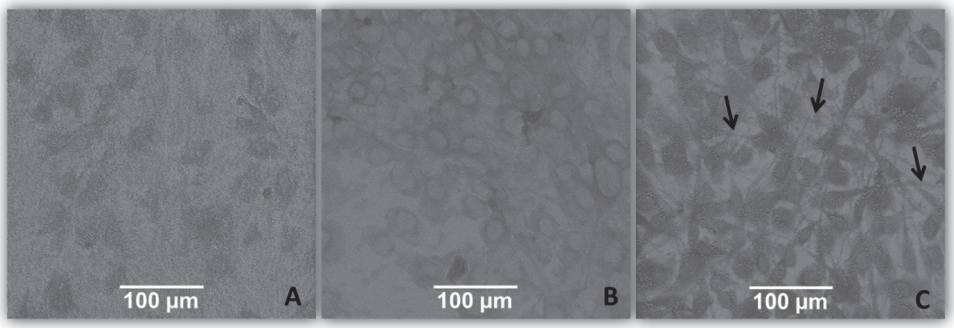

Fig. 4 SEM using variable pressure images in a 24 h period. (A) hydroxyapatite ceramic; (B) commercial pure titanium; (C) zirconia ZirCAD

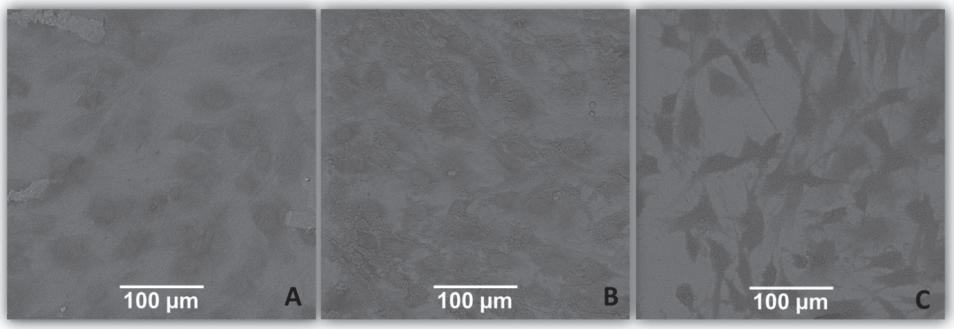

Fig. 5 SEM using variable pressure images at 48 h. (A) hydroxyapatite ceramic; (B) commercial pure titanium; (C) zirconia ZirCAD

eramic material studied became hydrophilic and consequently biologically favorable, as well as Ti, for osseointegration.

Biomaterials for dental implants should provide biocompatibility characteristics such as having no or low cytotoxicity, supporting cell differentiation and proliferation, and having good adhesion [28]. Cultures in microwells have a reduced cell growth area, resulting in suboptimal oxygen tension conditions and hydrogen ion diffusion potential, which are significantly different from those that are observed in conventional nutrient-scale cell cultures. As a result, cells maintained in these microenvironments may show abnormalities of basal metabolic activity and loss of viability due to nutritional stress, space limitations, and/or saturation of the medium; such implications may cause erroneous interpretation or low analytical sensitivity in assays applied to cell microcultures [29]. Therefore, the initial concentration of 2×10^3 cells/microwell and the selection of time intervals at 24 h, 48 h, and 72 h for viability tests were fundamental to the results, demonstrating the biocompatibility of the materials.

The results of the MTT assay reflected the activity of the mitochondrial enzymes. Therefore, if cell metabolism is unaffected by experimental treatments, the test provides information about metabolically active cells. When the initial quantity of cells is the same for all groups, and they have not been previously exposed to any toxic substance, the MTT assay can be used as an indirect marker of cell proliferation. Through the cell DNA pigment, the crystal violet assay confirmed the results found in the MTT assay.

In an indirect cell viability test, both in the MTT reduction assay and the crystal violet test, HC samples had similar behavior to the positive controls, which was considered to have 100% viability; that is, they showed no toxicity in any of the various dilutions or any of the various periods. The similarity was also evident in the comparison between the groups. Thus, it can be said that the dense HC that was developed does not cause death or injury to cells and can, therefore, be characterized as non-cytotoxic.

Although the occurrence of differences was statistically higher for Z-CAD zirconia and Ti in comparison to HC within the first 24 h in both cytotoxicity assays, for 48 h and 72 h, these differences did not remain, which demonstrated similarity in the final results of the material effects on cells (Figs. 2, 3).

The manufacture of dense $Ca_{10}(PO_4)_6(OH)_2$-containing additives, such as isopropyl alcohol dispersant PABA and PVB, together with an isostatic pressing pressure of 100 MPa for 30 s, resulted in apparent initial chemical stability and did not interfere with the metabolic activities of pre-osteoblast cells. Although in the case of pure $Ca_{10}(PO_4)_6(OH)_2$ having cationic and anionic substitutions, there may have been the ability to incorporate half of the periodic table elements in its structure [30]. In the process of osseointegration, this vulnerability can be beneficial for integration with the newly formed bone.

In addition, in relation to the manufacture of dense $Ca_{10}(PO_4)_6(OH)_2$, grain size is another factor that can influence the adhesion and proliferation of cells. In a study with a dense HC composite of different granulations ranging from microns to nanometers, Bose et al., in 2010, concluded that the grains that were thinner and smaller (on the order of 168 nm, 0.5 µm, and 1.16 µm) had better biological results as a consequence of increased contact with osteoblastic cells on the surfaces of these grains [31]. In the present study, the size of the grains used to construct the HC was around 0.35 µm, which is considered to be submicrometric, and this may have positively influenced the results.

The optimal properties of the starting powder, the sintering cycle, and the microstructure lead to adequate mechanical properties and biocompatibility. These are prerequisites for high-quality implant material [32]. This bovine HC was sintered at 1,300ºC and showed a tensile strength of 100 MPa and Vickers hardness of 4.5 GPa [Meira CR, Tese de Doutorado, Processamento de hidroxiapatita bovina associada com prototipagem rápida visando implantes ósseos, Universidade de São Paulo, 2014], which was above the minimum value for dense $Ca_{10}(PO_4)_6(OH)_2$ implants [33].

Although some studies have shown that the surface roughness of the materials positively influenced cell adhesion, differentiation, and consequently osseointegration, this study, which considered direct viability, showed that, on polished surfaces and the materials they were compared to as standardization of the samples, HC has characteristics that favor the proliferation of cells. In a 2014 study, Cho et al. compared Ti and zirconia with different surface treatments, and they also found that the surfaces of these polished materials facilitated the proliferation of pre-osteoblast cells [34].

Pioneering studies on the characteristics of cells visualized by light microscopy have already demonstrated the existence of morphological changes when they are attached to a substrate. The entire process of adhesion and proliferation consists of cell attachment, filopodial growth, cytoplasmic web, cell mass flattening, and the growth of the peripheral cytoplasm fringes progressing sequentially [35]. In the present study, these changes in cell morphology were observed on the surface of the evaluated

materials (Figs. 4, 5).

Differentiation of pre-osteoblasts into osteoblasts is characterized by polarized cells with basophilic cytoplasm and spherical nucleus. Osteoblasts are cuboidal or slightly elongated, and they form a continuous cell layer on the surface [36]. This differentiation applied to all pre-osteoblast cell materials used in this study, which enabled the same level of bone regeneration.

Among studies on dental implants, there is a high concentration of pre-osteoblasts that optimized the surfaces of dental implants to increase and accelerate the osteoblastic response and thus, promoted osseointegration and shortened its duration. Creating micro-roughness and incorporating bioactive substances, such as calcium phosphate ($Ca_{10}(PO_4)_6(OH)_2$), calcium and magnesium ions, or bone morphogenic proteins, may enhance and accelerate bone formation around implants [37]. Therefore, there is an interest in making HC a basic material in the manufacture of dental implants.

Dental implants made of bioceramic (zirconia) are used to avoid the problems inherent in traditional implants (metal, polymer), such as the release of ions and/or bone fracture (the gradient of elastic modulus), or the sensitivity of the organism to most foreign materials, which can result in the formation of a non-adherent layer of fibrous material around the implant [38]. Therefore, what is expected with future studies involving HC is to improve its mechanical properties and combine them with other materials that harmonize with biocompatibility, osteoconductivity and bioactivity.

Acknowledgments

This work was supported by the São Paulo Research Foundation (FAPESP) #2011/18061-0, #2012/06738-9, #2012/07283-5, and 2018/23639-0.

Conflict of interest

None declared.

References

1. Vale P, Gibbs H, Vale R, Munger J, Brandão A Jr, Christie M et al. (2019) Mapping the cattle industry in Brazil's most dynamic cattle-ranching state: slaughterhouses in Mato Grosso, 1967-2016. PLoS One 14, e0215286.
2. Muliggwe SE, Kaseva ME (2006) Assesssment of industrial solid state wast management and resource recovery pratices in Tanzania. Resources, Conservation and Recycling 47, 260-276.
3. Rodrigues CV, Serricella P, Linhares AB, Guerdes RM, Borojevic R, Rossi MA et al. (2003) Characterization of a bovine collagen-hydroxyapatite composite scaffold for bone tissue engineering. Biomater 24, 4987-4997.
4. Bagambisa FB, Joos U, Schilli W (1993) Mechanisms and structure of the bond between bone and hydroxyapatite ceramics. J Biomed Mater Res 27,1047-1055.
5. Chevalier J, Gremillard L (2009) Ceramics for medical applications: a picture for the next 20 years. J Eur Ceram Soc 29,1245-1255.
6. Zhuang Z1, Fujimi TJ, Nakamura M, Konishi T, Yoshimura H, Aizawa M (2013) Development of a, b-plane-oriented hydroxyapatite ceramics as models for living bones and their cell adhesion behavior. Acta Biomater 9, 6732-6740.
7. Veljovic DJ, Jokic B, Jankovic-Castvan I, Smiciklas I, Petrovic R, Janackovic DJ (2007) Sintering behaviour of nanosized HAP powder. Key Eng Mater 330-332, 259-262.
8. Veljovic DJ, Jokic B, Petrovic R, Palcevskis E, Dindune A, Mihailescu IN et al. (2009) Processing of dense nanostructured HAP ceramics by sintering and hot pressing. Ceram Int 35, 1407-1413.
9. Xu JL, Khor KA, Sui JJ, Chen WN (2009) Preparation and characterization of a novel hydroxyapatite/carbon nanotubes composite and its interaction with osteoblast-like cells. Mater Sci Eng C 29, 44-49.
10. Lukić M, Stojanović Z, Škapin SD, Maček-Kržmanc M, Mitrić M, Marković S et al. (2011) Dense fine-grained biphasic calcium phosphate (BCP) bioceramics designed by two-step sintering. J Eur Ceram Soc 31, 19-27.
11. Veljovic DJ, Jancic-Hajneman R, Balac I, Jokic B, Putic S, Petrovic R et al. (2011) The effect of the shape and size of the pores on the mechanical properties of porous HAP-based bioceramics. Ceram Int 37, 471-479.
12. Hacking AS, Harvey E, Roughley P, Tanzer M, Bobyn J (2008) The response of mineralizing culture systems to microtextured and polished titanium surfaces. J Orthop Res. 26, 1347-1354.
13. Jarcho M, Kay JK, Gumaer KI, Doremus RH, Drobeck HP (1977) Tissue, cellular and subcellular events at a boneceramic interface. J Bioengineering 1,79-92.
14. Ziats NP, Miller KM, Anderson JM (1988) In vitro and in vivo interactions of cells with biomaterials. Biomaterials 13, 5-13.
15. Chen S, Li L, Zhao C, Zheng J (2010) Surface hydration: principles and applications toward low-fouling/nonfouling biomaterials. Polymer 51, 5283-5293.
16. Charnley M, Textor M, Acikgoz A (2011) Designed polymer structures with antifouling-antimicrobial properties. React Funct Polym 71, 329-334.
17. Lourenço BN, Marchioli G, Song W, Reis RL, van Blitterswijk CA, Karperien M et al. (2012) Wettability influences cell behavior on superhydrophobic surfaces with different topographies. Biointerphases 7, 46.
18. Wu S, Liu X, Gao C (2015) Role of adsorbed proteins on hydroxyapatite-coated titanium in osteoblast adhesion and osteogenic differentiation. Sci Bull 60, 691-700.
19. Tagaya M, Yamazaki T, Tsuya D, Sugimoto Y, Hanagata N, Ikoma T (2011) Nano/microstructural effect of hydroxyapatite nanocrystals on hepatocyte cell aggregation and adhesion. Macromol Biosci 11, 1586-1593.
20. Abe Y, Okazaki Y, Hiasa K, Yasuda K, Nogami K, Mizumachi W et al. (2013) Bioactive surface modification of hydroxyapatite. Biomed Res Int 2013, 1-9, ID 626452.
21. Song YH, An JH, Seo YW, Moon WJ, Park YJ, Song HJ (2014) Osteoblast cell adhesion and viability on nanostructured surfaces of porous titanium oxide layer. J Nanosci Nanotechnol 14, 5682-5687.
22. Surmeneva MA, Kleinhans C, Vacun G, Kluger PJ, Schönhaar V, Müller M et al. (2015) Nano-hydroxyapatite-coated metal-ceramic composite of iron-tricalcium phosphate: Improving the surface wettability, adhesion and proliferation of mesenchymal stem cells in vitro. Colloids Surf B Biоint 135, 386-393.
23. Ferraris S, Vitale A, Bertone E, Guastella S, Cassinelli C, Pan J et al. (2016) Multifunctional commercially pure titanium for the improvement of bone integration: multiscale topography, wettability, corrosion resistance and biological functionalization. Mater Sci Eng C Mater Biol Appl 60, 384-393.
24. Pires LA, de Azevedo Silva LJ, Ferrairo BM, Erbereli R, Lovo JFP, Ponce Gomes O et al. (2020) Effects of ZnO/TiO2 nanoparticle and TiO2 nanotube additions to dense polycrystalline hydroxyapatite bioceramic from bovine bones. Dent Mater 36, 38-46.
25. Pagin MT, Oliveira FA, Oliveira RC, Sant'Ana AC, Rezende ML, Greghi SL et al. (2014) Laser and light-emitting diode effects on pre-osteoblast growth and differentiation. Lasers Med Sci 29, 55-59.
26. International Standards Organization (2009) Biological evaluation of medical devices-part 5: tests for in vitro cytotoxicity. ISO 10993-5:2009, Geneva.
27. Mosmann TA (1983) Rapid colorimetric assay for cellular growth and survival: application to proliferation and cytotoxicity assays. J Immunol Methods 65, 55-63.
28. Schmalz G, Arenholt-Bindslev D (2007) Biocompatibility of dental materials. Dent Clin N Am 51,747-60.
29. Olsson I, Johansson E, Bertnsson M, Eriksson L, Gottfries J, Wold S (2006) Rational DOE protocols for 96-well plates. Chemometr Intell Lab Syst 83, 66-74.
30. Rey C, Combes C, Drouet C, Sfihi H, Barroug A (2007) Physico-chemical properties of nanocrystalline apatites: implications for biominerals and biomaterials. Mater Sci Eng C 27, 198-205.
31. Bose S, Dasgupta S, Tarafder S, Bandyopadhyay A (2010) Microwave-processed nanocrystalline hydroxyapatite: simultaneous enhancement of mechanical and biological properties. Acta Biomat 6, 3782-3790.
32. Wei K, Li Y, Kim K-O, Nakagawa Y, Kim B-S, Abe K et al. (2011) Fabrication of nano-hydroxyapatite on electrospun silk fibroin nanofiber and their effects in osteoblastic behavior. J Biomed Mater Res A 97, 272-280.
33. Ravaglioli A, Krajewski A, Biasini V, Martinetti R, Mangano C, Venini G (1992) Interface between hydroxyapatite and mandibular human bone tissue. Biomaterials 13, 162-167.
34. Cho YD, Shin JC, Kim HL, Gerelmaa M, Yoon HI, Ryoo HM et al. (2014) Comparison of the Osteogenic Potential of Titanium and Modified Zirconia-Based Bioceramics. Int. J Mol Sci 15, 4442-4452.
35. Rajaramam R, Rounds DE, Yen SPS, Rembaum A (1974) A scanning electron microscope study of cell adhesion and spreading in vitro. Exptl Cell Res 88, 327-339.
36. Cerri PS (2005) Osteoblasts engulf apoptotic bodies durin alveolar bone formation in the rat maxilla. Anat Rec A Discov Mol Cell Evol Biol 286, 833-840.
37. Albrektsson T, Sennerby L, Wennerberg A (2008) State of the art of oral implants. Periodont 2000 47, 15-26.
38. Hench LL, Orcel G (1986) Physical-chemical and biochemical factors in sílica sol-gels. J Non-Crystal Sol 82, 1-10.